Heavy Precipitation Systems in the Mediterranean: The Role of the GPM

A.C. Marra[1], G. Panegrossi[1], P. Sanò [1], L.P. D'Adderio[1], S. Dietrich[1], L. Baldini[1], D. Casella[2], F. Porcù [3]

[1] CNR-ISAC, Rome, Italy; [2] SERCO S.p.A, Frascati, Italy; [3] Department of Physics and Astronomy, University of Bologna, Bologna, Italy

e-mail: g.panegrossi@isac.cnr.it

Introduction

Three examples of typical precipitation systems occurring in the Mediterranean area, that often devastate the coastal regions, are described and analyzed here by exploiting active and passive microwave measurements and state of the art precipitation products available in the GPM mission era. They are 1) a small-scale, and rapidly evolving, intense self-regenerating thunderstorm causing flashfloods; 2) a MCS leading to an exceptionally intense hailstorm; 3) a Mediterranean Tropical-Like Cyclone (or Medicane). The GPM key role in integrating observational ground-based and satellite-borne tools not only for precipitation monitoring, but also for understanding and characterizing severe weather in the Mediterranean, is described.

Isolated Deep-convection Systems: Livorno Flood

In the night between 9 and 10 Sept. 2017 a flash flood hit the coastal city of Livorno (lat 43.5°N, lon 10.3°E), Tuscany, causing damages and casualties. In the area around the city (black box in Fig.1), three raingauge stations measured over 230 mm of cumulated precipitation between 00 and 06 UTC of 10 Sept., with peaks of 75 mm in 30 minutes (150 mm h^{-1}) registered between 01 and 03 UTC.

12 overpasses of the GPM constellation MW radiometers (6 AMSU/MHS, 2 GMI, 2 SSMIS, 1 AMSR2, 1 ATMS) captured the storm throughout its transition over the area. As far as GPM Core Observatory (GPM-CO) overpasses, unfortunately DPR swath did not cover the storm, but GMI brightness temperatures (TBs) provided unique multichannel images of the mature cell over the city of Livorno (Fig.2).

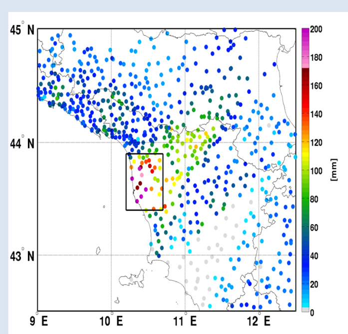

Fig.1: 24-h cumulated precipitation measured by the Italian raingauge network between 9 Sept. 12 UTC and 10 Sept. 12 UTC.

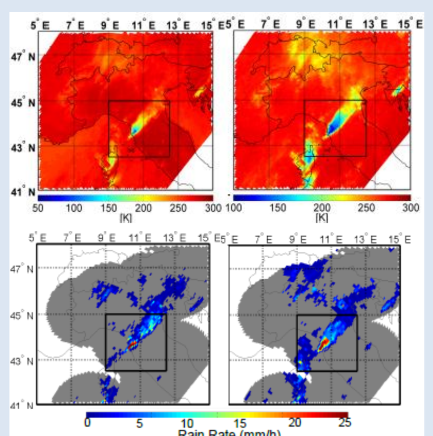

Fig.2: GPM-CO overpass at 01:17 UTC 10 Sept. GMI TBs at 89 GHz (V-pol) (top-left panel) and 166 GHz (V-pol) (top-right panel), DPC radar surface rainfall map at 01:20 UTC (bottom-left panel), and H SAF PNPR-GMI rainfall rate (RR) estimate (bottom-right panel) over the area covered by the radar. Black-box shows the area of Fig. 3.

The 24-h cumulated precipitation on 0.1°×0.1° grid (Fig.3) was obtained from:

1. Raingauges (from the Italian Department of Civil Protection - DPC), by cumulating half-hourly rainfall maps;
2. Ground-based Italian radar network mosaic (from the DPC), by integrating the surface rainfall maps available every 10 min;
3. PMW-only products (H SAF and GPM GPROF V05), by regridding RR retrievals available in the 24 h, assuming RR constant between two subsequent overpasses (Panegrossi et al., 2016);
4. MW/IR combined products (H SAF H03 and IMERG V05) by integrating the (mean) instantaneous RR estimates available every 15 and 30 min, respectively.

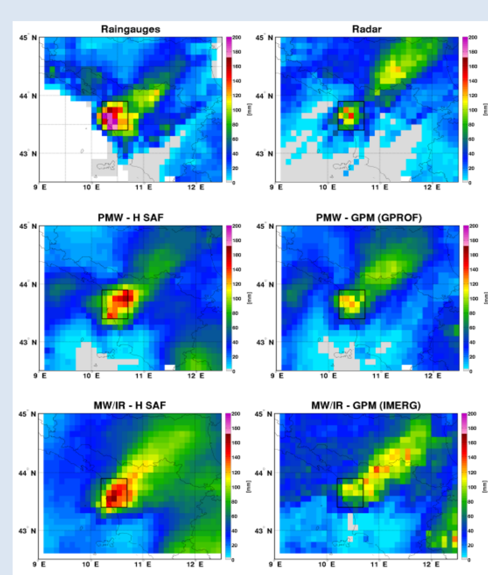

Fig.3: 24-h (12 UTC 9 Sept. - 12 UTC 10 Sept. 2017) cumulated precipitation. Raingauges and radar (top panels), PMW (H SAF and GPM) products (middle panels), and MW/IR (H SAF H03 and GPM IMERG Early V05) products. All the products are NRT, not calibrated to ground-based data, regridded on a 0.1°x0.1° grid, consistently with IMERG.

We notice:

- disagreement between raingauges and radars, especially in the region affected by the flood (black box in Fig. 1 and Fig. 3), with a significant (~50% on average) underestimation by the radar.
- striking difference between the 24-h precipitation maps obtained from H SAF and NASA products.
  - ✓ H SAF PMW products delineate quite well the area of intense precipitation with 20% underestimation and shift to the north-east compared to the raingauges.
  - ✓ H SAF MW/IR combined product (H03) has a similar behavior, with a well defined area of intense precipitation (slightly underestimated), and overestimation of the light to moderate precipitation and a tendency to falsely detect light precipitation.
  - ✓ NASA products, both GPROF and IMERG, show significant underestimation of the precipitation peak compared to the raingauges, but they are able to depict the light precipitation areas better than H SAF products.

It is worth noting that, while NASA GPM products are global, H SAF products are optimized for the Mediterranean area (except PNPR for GMI which is global)

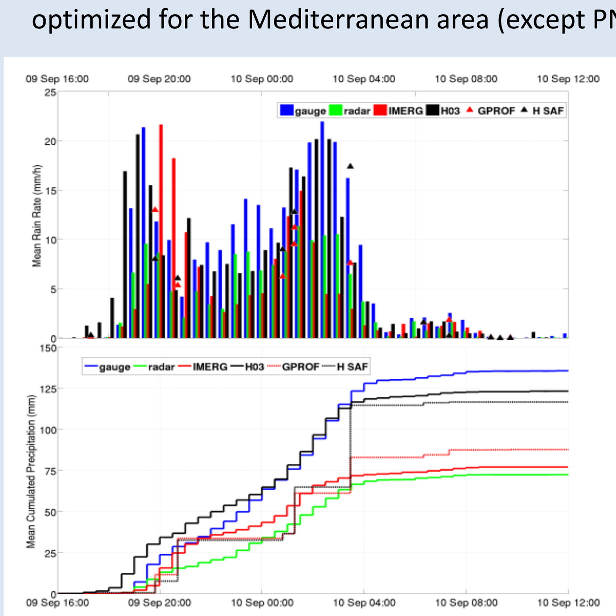

Fig. 4: Temporal evolution of the mean instantaneous precipitation (top panel) and mean cumulated precipitation (bottom panel), over the Livorno area (black box in Fig.3). Mean instantaneous precipitation rates available from the PMW products (H SAF and GPROF) for all radiometers, shown along with the half-hourly rainfall rates available from the MW/IR products (H03 and IMERG), and from raingauges and radars (top panel); corresponding curves of the mean cumulated precipitation (bottom panel).

The temporal evolution of the mean instantaneous precipitation (Fig.4, top panel) shows in details what already observed in Fig.3:

- the mean cumulated precipitation estimated by the radar is roughly 50% lower than the raingauges;
- H SAF and GPM products show an overall agreement in terms of instantaneous precipitation except at 03:28 UTC Sept. 10 (F16 SSMIS overpass) - H SAF estimate almost twice that from GPROF and radar, but in good agreement with the raingauges (discrepancy may be related to the missing high-frequency channels in F16 SSMIS data used as input by GPROF).
- H03 product follows quite closely the temporal evolution of the precipitation, in good agreement with the raingauges;
- IMERG seems to either follow or anticipate the peaks, in better agreement with the radar.

These results underlie the difficulties in getting reliable reference rainfall maps in case of small-scale, and rapidly evolving, intense events. On the other hand, despite the relatively poor performance of some products, they highlight the presence of a (at least qualitative) signature of the severity of the event in some of the satellite signals, making spaceborne sensors (not primarily designed for this application) useful in studying and monitoring such small scale/high impact events, whose occurrence at mid-latitude seems to increase in a climate change scenario.

MCS: The Naples hailstorm

Marra et al. (2017) analyzed one hailstorm that developed over the Tyrrhenian Sea and hit the Gulf and the city of Naples, in Italy, on 5 Sep. 2015 (hereinafter referred to as the Naples hailstorm), using GPM-CO observations in conjunction with other satellite and ground-based measurements. Here we present some of the analyses carried out by Marra et al. (2017), but based on the latest version (V05) of all the GPM products.

Three overpasses (two by MHS and one by the GPM-CO) captured the storm while it was off the coast and over the city of Naples. The GPM-CO overpass captured the mature phase of the storm (08:47 UTC) and provided unique spaceborne measurements of the 3-D structure of precipitation, evidencing extremely rare features of the Naples hailstorm.

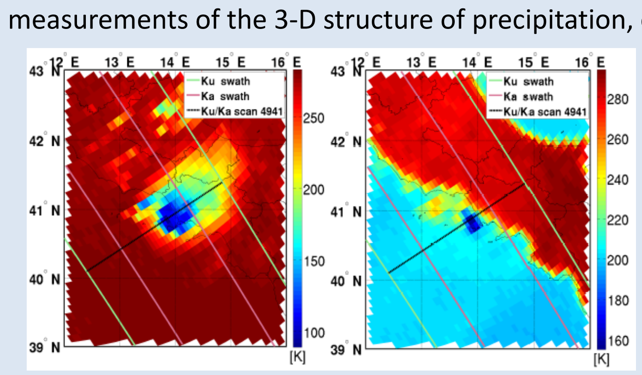

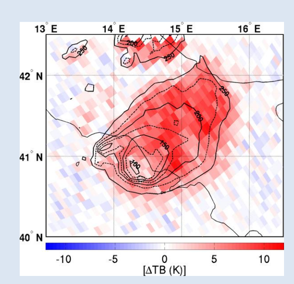

Fig. 5: Naples hailstorm on 5 September 2015 at 08:47 UTC. TBs at 166 GHz (V-pol) (top left panel) and TBs at 19 GHz (V-pol) (top right panel) and polarization difference (V-H) at 166 GHz (bottom panel) for GMI orbit 8630. Ku- and Ka-band DPR swaths are evidenced in green and magenta. The position of DPR-Ku scan 4941 (cross-section shown in Fig. 7) is shown in black.

- A deep GMI TB depression at 19 GHz (Fig.5 top right panel) clearly identifies the convective core of the hailstorm and is linked to the presence of very large hail;
- GMI 166 GHz TBs (Fig.5 top left panel) provide useful information on the different nature of the ice hydrometeors in the outflow region with respect to the convective core.
- The minimum TBs at 166 GHz, 20 K higher than at 89 GHz (not shown), are a clear indication of the presence of large, high-density ice particles at different levels of the updraft region.
- The GMI 166 GHz polarization difference (Fig.5 bottom panel) indicate a complex physical structure in the upper cloud layers, with different hydrometeor characteristics: randomly oriented/tumbling ice particles in the convective core, non-spherical ice crystals, with preferential horizontal orientation, in the convective outflow region.

DPR measurements provide further support to the GMI analysis.

- The values of the reflectivity factor measured at Ku-band (Z_m) around 50 dBZ indicate the presence of hail;
- The map of DPR Ku-band median corrected reflectivity factor Z_c (V05A), with superimposed LINET strokes [Intra-Cloud (IC) and Cloud-to-Ground (CG)] (Fig. 6 left panel), highlights that most of the strokes are concentrated within the area of maximum Z_c (coincident with the area of minimum TBs at 19 GHz).
- For this exceptional case (Iguchi et al., 2018), all the different methods, by which the "heavy ice precipitation" flag (available in DPR product V05) is defined, detect the occurrence of heavy ice precipitation within the cell core (Fig.6 right panel). This area includes the area of minimum TB at 19 GHz (V-pol) shown in Fig. 5.

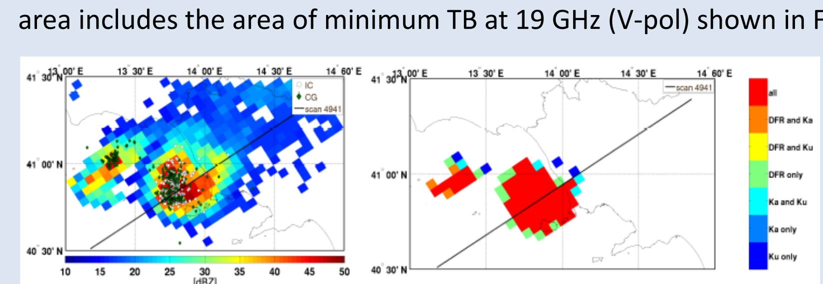

Fig. 6: Left panel: DPR Ku-band median Z_c and LINET strokes (IC and CG) registered during a 4 min time interval around 08:47 UTC (left panel), with the position of DPR-Ku scan 4941 shown in Fig. 7 (black line); Right panel: heavy ice precipitation flag available in the JAXA DPR V05 products determined with different criteria. A hook echo associated with mesocyclone is noticeable in Ku-band reflectivity (it is very well defined in the ground C-band radar image shown in Marra et al., 2017).

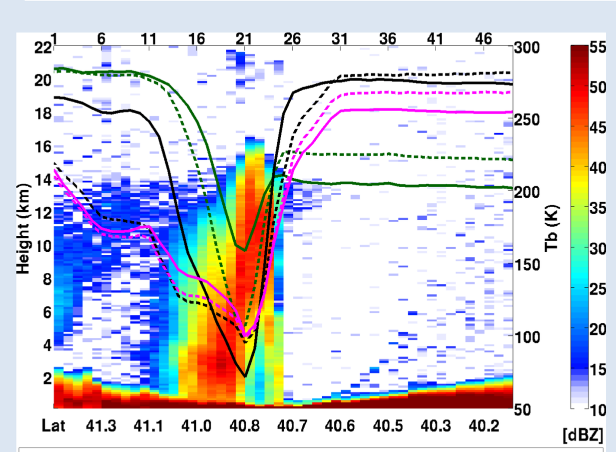

Fig.7: Across-track scan 4941 of DPR Ku Z_m. GMI TBs 4 window channels (V-Pol) and 183.31 GHz channels, corrected for parallax effects, are superimposed. On top the DPR Ku-band ray number along the cross-section is indicated.

DPR Ku Z_m cross section (Fig. 7) along the most intense portion of the storm (black line in Fig.5 and 6) reveals

- an overshooting top height at 16.25 km a.s.l.
- a slanted structure of the main updraft, sign of vertical wind shear and storm severity, associated with the hook-echo shown in Fig. 6.
- strong attenuation, and mirror echo at 22 km a.s.l.

Z_m shows a well-defined structure of the storm, including the anvil and the main deep convective core, where the TBs reach extremely low values (158 K, 97 K, 67 K, and 87 K at 19, 37, 89 and 166 GHz respectively).

The high values of Z_m (~55 dBZ at 10 km, 40 dBZ echo top height at 14-15 km) indicate the presence of a very intense core of high-density ice particles (hail), maintained by a very strong updraft, in the upper levels.

Analysis of Precipitation Features (PFs) (Liu and Zipser, 2015) found in 49 months of GPM global observations (http://atmos.tamucc.edu/trmm/data/gpm) confirms the severity and exceptionality of the Naples hailstorm at global scale in terms of minimum TBs (or Polarization Corrected Temperature, PCT), with the lowest 19 GHz TB minimum (V-pol) (158 K) measured in the Northern Hemisphere for the period analyzed (Table 1).

GMI	Rank	Tropics	Mediterranean	CONUS	Other
19 GHz	2	-	1 (50%)	-	1 (50%)
23 GHz	4	-	1 (25%)	2 (50%)	1 (25%)
37 GHz	7	-	1 (14%)	4 (57%)	2 (29%)
89 GHz	161	138 (85.71%)	3 (1.86%)	16 (10%)	4 (2.5%)

Table 1. PFs found in 49 months of GPM observations (03/2014-03/2018, http://atmos.tamucc.edu/trmm/data/gpm) based on minimum TB values. Ranking of Naples hailstorm (for each TB) with respect to over 28 millions (28,204,150) global PFs (second column). Geographical distribution (in terms of number and %) of the PFs with TB minimum values equal to or lower than those found for the Naples hailstorm (third to sixth column).

Specific studies, carried out to find a relationship between minimum TBs and hail, confirm that the remarkable low TBs at low frequencies (noteworthy at 19 GHz), found for the Naples hailstorm, are linked to the large size of the convective core of the storm, and to the presence of large massive ice particles (8-10 cm diameter) sustained at upper levels by very strong updraft.

Mediterranean Tropical-like Cyclones: Numa

Numa was classified as hybrid storm with both tropical and sub-tropical characteristics by NOAA/NESDIS, and as a Mediterranean Hurricane (Medicane) by EUMETSAT.

The storm started to develop over the Strait of Sicily, on Nov. 15, 2017, and it deepened moving eastward on Nov. 16. Then it moved across the relatively warm Ionian Sea towards the Southern Apulia region in Italy (12UTC 17 Nov. – 12UTC 18 Nov.) where it revealed TLC structure (well-defined, quasi cloud-free, eye surrounded by a whirl of clouds). It persisted over the coast of Apulia maintaining its TLC features for 24 h causing extensive floods and damages (raingauge peaks of 165 mm in 24 h). Then it moved eastward, and completely dissipated over Greece on 19 Nov. (Fig.8 top panel). The damages were due not to the rainfall intensity (mostly between 5 and 10 mm/h), but to the persistency. Lightning activity is more intense during the development phase (Fig.8 bottom panel) than during its TLC phase confirming what was found by Miglietta et al. (2013).

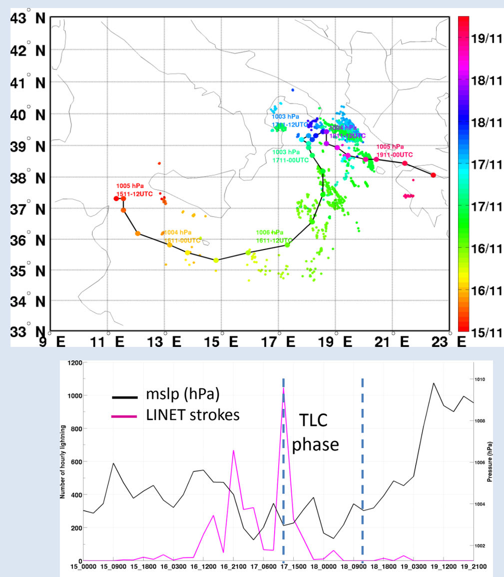

Fig. 8: ECMWF minimum MSLP and total LINET strokes within a 200 km radius from the TLC center in 1 hour: track (top panel) and temporal evolution (bottom panel).

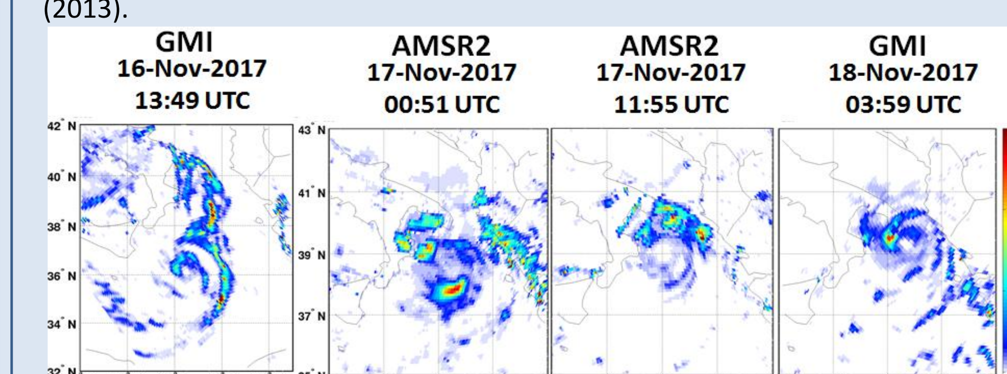

Fig.9: Surface precipitation rate estimated by the GPROF V05 algorithm for four Numa overpasses by AMSR2 (middle panels) and GMI (left and right panels).

- 53 GPM constellation overpasses in four days (15 -19 Nov.) are available, mostly when the storm is over the sea and no other observations of precipitation are available (15 overpasses during the TLC phase);
- Two GPM-CO overpasses,
  - ✓ one during Numa development phase on 16 Nov. 13:49 UTC, when the storm is captured by both GMI and DPR (Fig. 10);
  - ✓ one during its mature phase on 18 Nov. 03:59 UTC, when it is captured only by GMI.

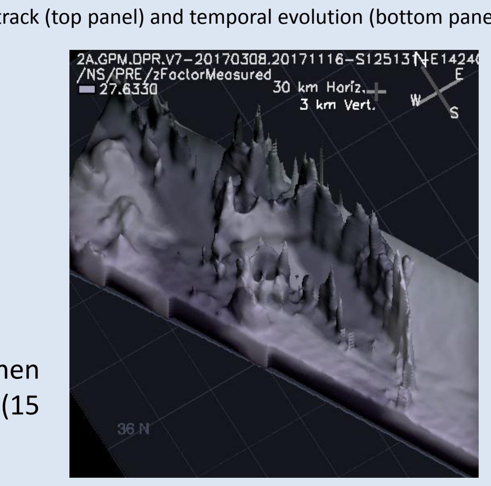

Fig.10: DPR Ku Z_m from the GPM-CO overpass of Numa during its development phase on 16 Nov. 2017, 13:49 UTC.

GPROF (V05) RR estimates (Fig. 9) highlights how the precipitation structure evolves during the different stages of the storm development. During the initial phase, less organized structure, with regions of lighter and heavier rainfall coexist, while a well-defined eye and rainband structure can be observed during the mature phase.

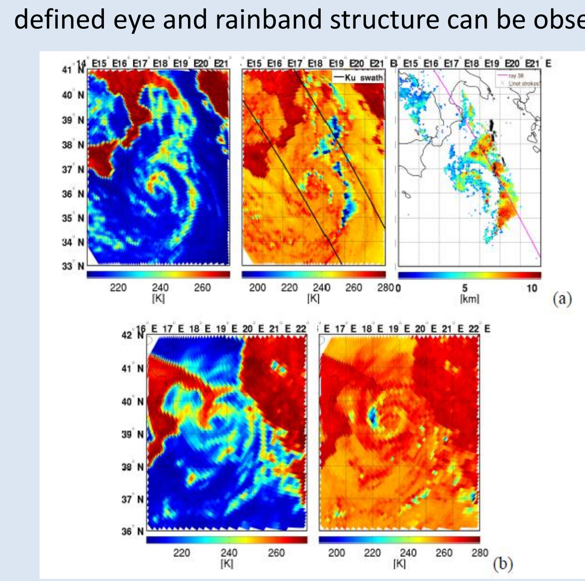

Fig.11. (a) GPM-CO overpass on Nov. 16, 13:50 UTC. Left panel: 37 GHz GMI TB. Middle panel: 89 GHz GMI TB. Right panel: CTH (km), with LINET strokes registered in 1 hour around the overpass time shown by black crosses. (b) GPM-CO overpass on Nov. 18, 03:59 UTC. Left panel: GMI TB at 37 GHz. Right panel: GMI TB at 89 GHz. The black line in the top-right panel shows the position of the cross-section along Ray 38 (Fig. 12)

The differences in the rainbands' morphology between the development and the mature phase of Numa are clearly visible in Fig.11, where GMI TBs at 37 GHz and 89 GHz are compared.

- The GMI 37 GHz channel is able to depict very well the fine structure of the rainbands. TBs are well correlated to the surface RR shown in Fig. 9.
- The absence of scattering signal at this frequency (often visible in presence of deep convection, in the areas of lower 89 GHz TBs), evidences moderate (shallow) convective activity.
- The weak scattering signal at 89 GHz, corresponding to the main rainbands, is a further evidence of the presence of low clouds, likely consistent with a slanted eyewall (as reported by Miglietta et al., 2013).
- The lowest 89 GHz TBs (~190 K) are found in correspondence of the convective regions. Convection characterizes most part of the rainbands during the development phase, while it is confined to the western portion of the eyewall during the mature phase.

The DPR Cloud Top Height (CTH, Fig. 11, top-right panel), reconstructed from the Ku-band Z_m, as well as the Ku-band Z_c cross section (Fig. 12, top panel) shows that the maximum height during the development phase ranges between 6 km and 10 km, with taller clouds mostly located on the eastern side of the cyclone center, confirming what was inferred from GMI TBs. Electrical activity is concentrated in the areas of higher CTH (and minimum TBs at 89 GHz). Large D_m (Fig. 12, bottom panel) is found in correspondence of the convective core (at 36.7°N – 18.8°E), exceeding 3 mm also in the upper cloud layers (up to 6-7 km). A stratiform region (36.1°N-19.3°E) is evidenced by a clear signal of bright-band (peak of Z_c) in close correspondence with the freezing level height (~2400 m) as inferred from the ECMWF analysis. Lower (up to 2 mm) and nearly constant D_m values are found in this region.

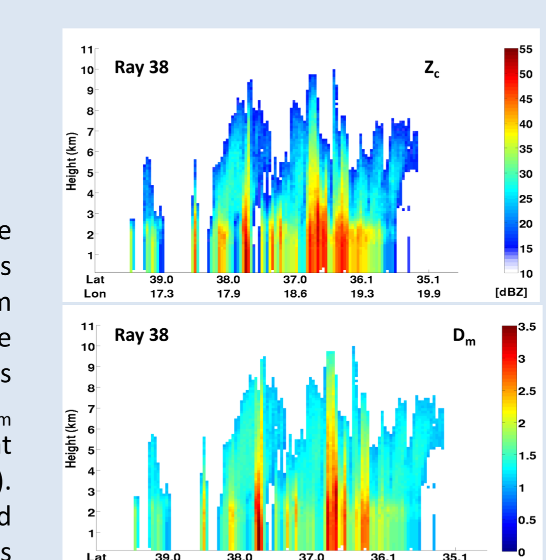

Fig. 12: Cross section along ray 28 of Z corrected at Ku-band and mass-weighted mean diameter (from 2ADPR-NS product V05)

Conclusions

We presented three events that have recently challenged observational and forecasting capabilities in the Mediterranean, and caused damages at the ground. Making use of ground-based and satellite-borne instruments, we addressed the problem of estimating precipitation of a small-scale and short-living intense thunderstorm, the capability to render the 3D structure of a mesoscale convective system, and the key role of satellite view in the classification and monitoring of a Medicane. Measurements and precipitation products available in the GPM era can be successfully exploited with the aim to increase the knowledge of severe systems in the Mediterranean area and to support operational forecasting activities in this complex region in a climate change perspective.

To fully achieve this purpose, efforts should be undertaken to provide products tailored for this regions (working on algorithm calibration), and provide the error structure of the products (working on validation). This would enable users to properly apply the more suitable product for the specific need, including data assimilation of precipitation-related fields over the sea where heavy precipitation systems affecting the Mediterranean coastal regions often initiate. Moreover, long data records of satellites precipitation-related measurements and reliable products would help assessing climate change signatures in the Mediterranean area, where such severe events are becoming more and more frequent.

References

Iguchi, T., Kawamoto, N., Oki, R., 2018: Detection of Intense Ice Precipitation with GPM/DPR. *J. Atmos. Oceanic Technol.*, **35**, 491–502. https://doi.org/10.1175/JTECH-D-17-0120.1

Liu, C., Zipser, E. J., 2015: The global distribution of largest, deepest, and most intense precipitation systems. *Geophys. Res. Lett.*, **42**, 3591–3595. https://doi.org/10.1002/2015GL063776

Marra, A.C., Porcù, F., Baldini, L., Petracca, M., Casella, D., Dietrich, S., Mugnai, A., Sanò, P., Vulpiani, G., Panegrossi, G., 2017: Observational analysis of an exceptionally intense hailstorm over the Mediterranean area: Role of the GPM Core Observatory. *Atmospheric Research*, **192**, 72-90, ISSN 0169-8095. https://doi.org/10.1016/j.atmosres.2017.03.019.

Miglietta, M.M., Laviola, S., Malvaldi, A., Conte, D., Levizzani, V., Price, C., 2013: Analysis of tropical-like cyclones over the Mediterranean Sea through a combined modelling and satellite approach. *Geophys. Res. Lett.* **40**, 2400–2405. https://doi.org/10.1002/grl.50432

Panegrossi, G., Casella, D., Dietrich, S., Marra, A.C., Petracca, M., Sanò, P., Mugnai, A., Baldini, L., Roberto, N., Adirosi, E., Cremonini, R., Bechini, R., Vulpiani, G., Porcù, F., 2016: Use of the GPM constellation for monitoring heavy precipitation events overthe Mediterranean region. *IEEE JSTARS*, **9**, 2733–2753. http://dx.doi.org/10.1109/JSTARS.2016.2520660.

Acknowledgements

This research was supported by the EUMETSAT "Satellite Application Facility on Support to Operational Hydrology and Water Management" (H-SAF)) CDOP-3, by the Italian Research Project of National Interest 2015 (PRIN 2015) 4WX5NA, and by the DPC-ISAC Operational Agreement 2018. The PMM Research Program and EUMETSAT are warmly acknowledged for supporting H SAF and GPM collaboration through the approval of the no-cost H SAF-GPM proposal "H SAF and GPM: precipitation algorithm development and validation activity". The NASA PPS is warmly acknowledged for providing GPM products.